

# Comparison of Diagnostic Efficacy of Gd-EOB-DTPA-Enhanced MRI and Dynamic Contrast-Enhanced Multislice CT in Hepatocellular Carcinoma

Rumiko Kasai<sup>1)†</sup> Terumitsu Hasebe<sup>2)\*†</sup> Nobuo Takada<sup>3)</sup>  
Tsutomu Inaoka<sup>1)</sup> Nobuyuki Hiruta<sup>4)</sup> and Hitoshi Terada<sup>1)</sup>

<sup>1)</sup>Department of Radiology (Sakura), School of Medicine, Faculty of Medicine, Toho University

<sup>2)</sup>Department of Radiology, Tokai University Hachioji Hospital, Tokai University School of Medicine

<sup>3)</sup>Division of Gastroenterology and Hepatology, Department of Internal Medicine (Sakura), School of Medicine, Faculty of Medicine, Toho University

<sup>4)</sup>Department of Surgical Pathology (Sakura), School of Medicine, Faculty of Medicine, Toho University

## ABSTRACT

**Background:** Hepatocellular carcinoma (HCC) is a common cause of cancer death. In planning optimal treatment, it is important to determine accurately the number and size of HCC lesions. We compared the ability of gadolinium-ethoxybenzyl-diethylenetriamine-pentaacetic acid (Gd-EOB-DTPA)-enhanced magnetic resonance imaging (MRI) and dynamic contrast-enhanced computed tomography (CT) to detect HCC lesions in a clinical setting.

**Methods:** We retrospectively investigated the medical records of 47 consecutive patients (age  $65.4 \pm 9.1$  years; 74% men) with suspected focal liver lesions detected by ultrasonography, unenhanced CT, or elevated serum  $\alpha$ -fetoprotein levels. All patients had undergone both dynamic contrast-enhanced 64-multislice CT and Gd-EOB-DTPA-enhanced MRI. All images were examined by experienced independent radiologists and were compared with a final diagnosis that was based on all available clinical information and was determined via consensus. The McNemar test was used to compare the 2 imaging modalities in lesion-based analysis for the detection of HCC.

**Results:** Clinical, histopathologic, and radiologic follow-up revealed 58 HCC lesions in 24 patients. Dynamic contrast-enhanced CT and Gd-EOB-DTPA-enhanced MRI detected 43 and 54 HCC lesions, respectively; 39 lesions were detected by both modalities. The sensitivity was 74% for CT and 93% for MRI ( $p = 0.022$ ). Even when no lesion was detected by dynamic contrast-enhanced CT, Gd-EOB-DTPA-enhanced MRI depicted 15 hypointense lesions during the hepatobiliary phase, with very weak Gd-EOB-DTPA-enhancement during the early arterial phase. Moreover, 1 lesion showed a mixture of hypointensity and hyperintensity during the hepatobiliary phase of Gd-EOB-DTPA-enhanced MRI and was histologically diagnosed as a mixture of well-differentiated HCC and so-called green hepatoma.

**Conclusions:** The clinical sensitivity of Gd-EOB-DTPA-enhanced MRI was better than that of dynamic contrast-enhanced 64-multislice CT for diagnosis of HCC.

J Med Soc Toho 59 (6): 279–289, 2012

**KEYWORDS:** hepatocellular carcinoma, Gd-EOB-DTPA, MRI, dynamic contrast-enhanced CT, detectability

† Both authors equally contributed to this work  
1, 3, 4) 564-1 Shimoshizu, Sakura, Chiba 285-8741  
2) 1838 Ishikawa-machi, Hachioji, Tokyo 192-0032  
\*Corresponding Author: tel: 042(639)1144

e-mail: hasebe@hachioji-hosp.tokai.ac.jp  
Received May 22, 2012; Accepted Sept. 28, 2012  
Journal of the Medical Society of Toho University  
59 (6), Nov. 1, 2012. ISSN 0040-8670, CODEN: TOIZAG

Hepatocellular carcinoma (HCC) is the most common primary liver cancer and is becoming more prevalent worldwide.<sup>1,2)</sup> It is the third leading cause of cancer death and is responsible for more than 600000 deaths annually. Therapeutic options for HCC have markedly improved over the last 10 years and now include transcatheter arterial chemoembolization, transplantation, surgical resection, and local ablation.<sup>3)</sup> It is important to identify accurately the number, size, and location of hepatic lesions, and to provide a differential diagnosis that ensures selection of the most appropriate treatment.<sup>4)</sup> Imaging modalities are essential in establishing the correct diagnosis.<sup>5)</sup>

Recently, a variety of imaging modalities, including ultrasonography (US), computed tomography (CT), and magnetic resonance imaging (MRI), have been used to detect and diagnose HCC. Multiphasic helical CT is widely used for hepatic follow-up because of its low invasiveness, greater speed, high rate of use within hospitals, and superior spatial and temporal resolution.<sup>6-8)</sup> Due to the development of a variety of tissue-specific MRI contrast agents—*e.g.*, superparamagnetic iron oxide (which targets Kupffer cells) and gadobenate dimeglumine (which is weakly taken up by hepatocytes)—contrast-enhanced MRI of the liver is increasingly considered a more accurate imaging modality than multiphasic helical CT.<sup>9,10)</sup>

An innovative liver-specific MRI contrast agent, gadolinium-ethoxybenzyl-diethylenetriamine-pentaacetic acid (Gd-EOB-DTPA; EOB·Primovist® Inj. Syringe, Bayer Yakuhin, Ltd., Osaka, Japan), has recently been introduced in clinical imaging.<sup>11,12)</sup> Although studies have compared multiphase spiral CT and Gd-EOB-DTPA-enhanced MRI in the detection and characterization of HCC, the findings have differed. A recent study suggested that Gd-EOB-DTPA-enhanced MRI was more accurate than multiphase spiral CT in detecting hepatic lesions among blinded readers, although the results did not reach statistical significance. More noteworthy was a study showing that Gd-EOB-DTPA-enhanced MRI was superior to CT in detecting small HCC lesions.<sup>13,14)</sup> Other multicenter trials found that the proportion of lesions correctly characterized by Gd-EOB-DTPA-enhanced MRI was significantly higher than the proportion correctly characterized by biphasic CT. However, the enrollment of a highly selected population of patients with suspected malignant lesions was a limitation of these trials.<sup>15)</sup> In addition, the CT and MRI protocols differed in the same trial.<sup>16)</sup> The most recent study indicated that Gd-EOB-DTPA-enhanced MRI and

triple-phase multidetector CT had similar diagnostic performance in preoperative detection of HCC.<sup>17,18)</sup> We retrospectively compared the clinical performance of dynamic contrast-enhanced 64-multislice CT and Gd-EOB-DTPA-enhanced MRI in detecting HCC lesions among patients with suspected focal liver lesions.

## Methods

### 1. Patient characteristics

We retrospectively investigated the records of 47 consecutive patients (age  $65.4 \pm 9.1$  years; 74% men) with suspected focal liver lesions identified by US, unenhanced CT, or elevated serum  $\alpha$ -fetoprotein levels between April 2007 and August 2009. This study was designed to compare dynamic contrast-enhanced 64-multislice CT and Gd-EOB-DTPA-enhanced MRI in a routine clinical setting. Because 10% to 20% of HCC lesions develop in noncirrhotic liver or in patients with nonviral hepatitis, or are incidental thereto,<sup>2,19)</sup> we included patients with or without known hepatic disease. Of such patients, 35 were men (age range, 40-80 years; mean age, 67.8 years), and 12 were women (age range, 47-76 years; mean age, 64.5 years). All patients underwent triple-phase dynamic-enhanced 64-multislice CT and Gd-EOB-DTPA-enhanced MRI within a period of 6 weeks (mean interval, 10.4 days; range, 1-41 days), as described in previous reports.<sup>13,15,18)</sup> Our hospital ethics committee reviewed and approved the study protocol. Written informed consent was obtained from all patients. Exclusion criteria included presence of clinically unstable conditions, severe renal impairment, and refusal to participate in the study.

### 2. Liver-specific MRI contrast agent

Gd-EOB-DTPA is a gadolinium-based, paramagnetic, hydrophilic, ionic, highly water-soluble diagnostic contrast agent with dual elimination routes. Approximately 50% of the injected dose is taken up by functioning hepatocytes and excreted in bile; the remaining 50% is eliminated by renal excretion. It produces high T1 relaxivity in liver tissue immediately after contrast administration. Dynamic and accumulation (hepatospecific) phase imaging can also be performed after bolus injection of Gd-EOB-DTPA. Thus, information on lesion vascularity and cell composition can be obtained. HCC does not usually act on hepatocytes, so lesions appear as hypointense areas against healthy liver parenchyma in T1-weighted images. All patients received a 0.025-mmol per kg body weight dose of a 0.25-mol/l gadoteric acid solution administered via an an-

tecubital vein, with a flow velocity of 3 ml/s and flushing with 20 ml of 0.9% saline.<sup>11,13,20)</sup>

### 3. Imaging protocols

Dynamic-enhanced CT images were acquired within 6 weeks before or after Gd-EOB-DTPA-enhanced MRI in all patients. For triple-phase dynamic CT (Aquilion™ 64; Toshiba Medical Systems Corp., Otawara, Japan), after an initial scout scan, images were acquired before administration of contrast material (120 kV; 140-375 mA; section thickness: 1 mm; table speed: 27 mm/s; rotations: 0.5 per s; acquisition time: approximately 5 s; field of view: 300-425 mm). All patients received nonionic low-osmolar contrast material with an iodine concentration of 370 mg I/ml (Iopamiron 370®; Bayer Yakuhin, Ltd.) via an antecubital vein with a flow velocity of 3 ml/s, using a programmed CT injector. As in previous studies, the scans were obtained 35, 60, and 120 seconds after the start of the injection, during the arterial, portal, and equilibrium phases, respectively.<sup>21,22)</sup> The iodine dose used in this study was 516 mg I/kg body weight, based on the results of previous studies.<sup>23-25)</sup>

MRI examinations were performed at 1.5 T (Gyrosan Intera 1.5 T; Philips Medical Systems International B.V., Best, Netherlands). After initial scout images, the following images were obtained: axial T2-weighted single-shot turbo spin-echo (TSE) (TR = 403 ms; TE = 60 ms; 60° flip angle, 7-mm section thickness, 1-mm section gap), axial T1-weighted TSE (TR = 500 ms; TE = 69 ms; 70° flip angle, 7-mm section thickness, 0.7-mm section gap), and axial diffusion-weighted echo-planar (TR = 1746 ms; TE = 72 ms; 7-mm section thickness, 1-mm section gap, 1000 sec/mm<sup>2</sup> b-value). Thereafter, Gd-EOB-DTPA was administered intravenously and flushed with 20 ml of 0.9% saline. Arterial phase, portal venous phase, and equilibrium phase images were acquired 20, 60, and 120 seconds after contrast material administration, using a 3-dimensional gradient-echo (3D-GRE) sequence with fat suppression (TR = 4.9 ms; TE = 2.5 ms; 13° flip angle, 4-mm section thickness, no section gap). The dynamic study was followed by a delayed-phase axial imaging 2.5 minutes after injection of contrast material, with the same T1-weighted TSE protocol. Hepatospecific phase axial, sagittal, and coronal images were obtained 20 minutes later, using the same 3D-GRE protocol.

### 4. Reference diagnosis

The offsite interpretation of dynamic-enhanced CT images and Gd-EOB-DTPA-enhanced MR images were compared with the reference diagnosis, which was made on-

site by evaluating all available data for each patient. Image evaluations performed by 2 experienced independent radiologists were compared with the final diagnosis for HCC lesions, which was based on all available clinical information (including US, CT, MRI findings; laboratory data; histopathologic findings; and radiologic follow-up examinations) and was determined via consensus. Lesions suspected as HCC on the basis of results from more than 2 modalities and other clinical data, including data from follow-up examinations, were clinically diagnosed as HCC. Follow-up examinations were included in the clinical routine and were not part of the study protocol.

### 5. Statistical analysis

The sensitivity, specificity, and accuracy of dynamic-enhanced CT and Gd-EOB-DTPA-enhanced MRI were calculated using the reference diagnosis. The accuracies of dynamic-enhanced CT and Gd-EOB-DTPA-enhanced MRI for detection of HCC lesions were determined, and differences between the 2 modalities were evaluated using the McNemar test. A p value less than 0.05 was considered to indicate statistical significance.

## Results

### 1. Results of reference diagnosis

Regarding the reference diagnosis for all lesions, 24 patients had 58 HCC lesions, 8 patients had 16 metastases, 7 patients had 12 hemangiomas, 2 patients had 4 cysts, 2 patients had 2 hyperplastic nodules, and 2 patients had 20 cholangiocarcinomas. Histopathologic information was available for reference diagnosis for 8 of 115 detected lesions, among which 4 lesions were HCC.

### 2. Lesion detection and characterization

Dynamic-enhanced CT and Gd-EOB-DTPA-enhanced MRI detected 43 and 54 HCC lesions, respectively; 39 were detected by both modalities. There were 15 HCC lesions in 5 patients that were not detected by any observers on dynamic-enhanced CT images but were detected on Gd-EOB-DTPA-enhanced MR images (mean lesion size, 10.8 mm; Fig. 1). These 5 patients had 11 other HCC lesions that were revealed by both modalities. In contrast, there were 4 HCC lesions in 2 patients that were not detected by any observer on Gd-EOB-DTPA-enhanced MRI but were detected on dynamic-enhanced CT (mean lesion size, 15.3 mm; Fig. 2). These 2 patients had 7 other HCC lesions that were detected by both modalities. One patient had 1 false-positive lesion diagnosed as HCC on Gd-EOB-DTPA-enhanced MRI. The lesion was diagnosed as adenomatous

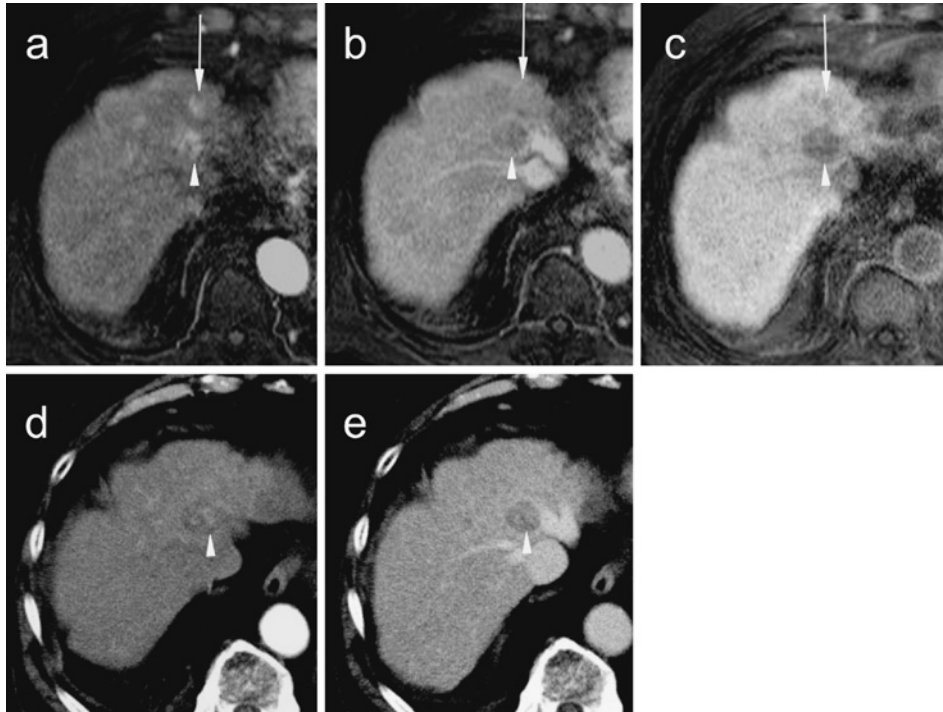


Fig. 1 An 80-year-old man with multiple HCC lesions.

- a. A T1-weighted Gd-EOB-DTPA-enhanced arterial phase MR image shows 2 hypervascular nodules in liver segment IV (arrow and arrowhead).
- b. A T1-weighted Gd-EOB-DTPA-enhanced equilibrium phase MR image shows washout pattern of 2 nodules in segment IV (arrow and arrowhead). The dorsal nodule shows a clear washout pattern (arrow) during this phase; however, the ventral lesion, which was recognized as a hypervascular nodule in a Gd-EOB-DTPA-enhanced arterial phase image, shows intermediate signal intensity.
- c. A T1-weighted Gd-EOB-DTPA-enhanced hepatobiliary phase MR image shows 2 hypointense nodules in segment IV (arrow and arrowhead).
- d. Contrast-enhanced CT scan during the arterial phase shows a 2.8-cm-diameter hypervascular HCC in segment IV (arrowhead). No lesion is visible on the ventral side of this nodule.
- e. A contrast-enhanced CT scan obtained during the equilibrium phase shows a washout pattern of HCC in segment IV (arrowhead). No lesion is visible on the ventral side of this nodule (false negative lesion on CT).
- HCC: hepatocellular carcinoma, Gd-EOB-DTPA: gadolinium-ethoxybenzyl-diethylenetriamine-pentaacetic acid, MR: magnetic resonance, CT: computed tomography

hyperplasia on dynamic-enhanced CT (no hypervascular lesion during the early arterial phase and a low-density lesion during the equilibrium phase) and was definitively diagnosed as nodular hyperplasia after surgery (Fig. 3). One lesion that was diagnosed as HCC by both modalities showed a mixture of hypointensity and hyperintensity in the hepatobiliary phase of Gd-EOB-DTPA-enhanced MRI (Fig. 4). This lesion was pathologically confirmed to be a well-differentiated HCC containing bile pigment, *i.e.*, a so-called green hepatoma.

### 3. Statistical analysis

On a per lesion basis, the sensitivity, specificity, and ac-

curacy of dynamic-enhanced CT in the detection of HCC were 74, 100, and 91%, respectively. The diagnostic sensitivity, specificity, and accuracy of Gd-EOB-DTPA-enhanced MRI were 93, 98, and 96%, respectively. The sensitivity of Gd-EOB-DTPA-enhanced MRI was significantly higher ( $p = 0.0218$ ) than that of dynamic-enhanced CT in detecting HCC (Table 1). Additionally, the accuracy of Gd-EOB-DTPA-enhanced MRI was significantly higher than that of dynamic-enhanced CT in detecting HCC ( $p < 0.001$ ). The positive predictive value and negative predictive value were 100% (43 of 43) and 79% (57 of 72), respectively, for dynamic-enhanced CT and 98% (54 of 55) and

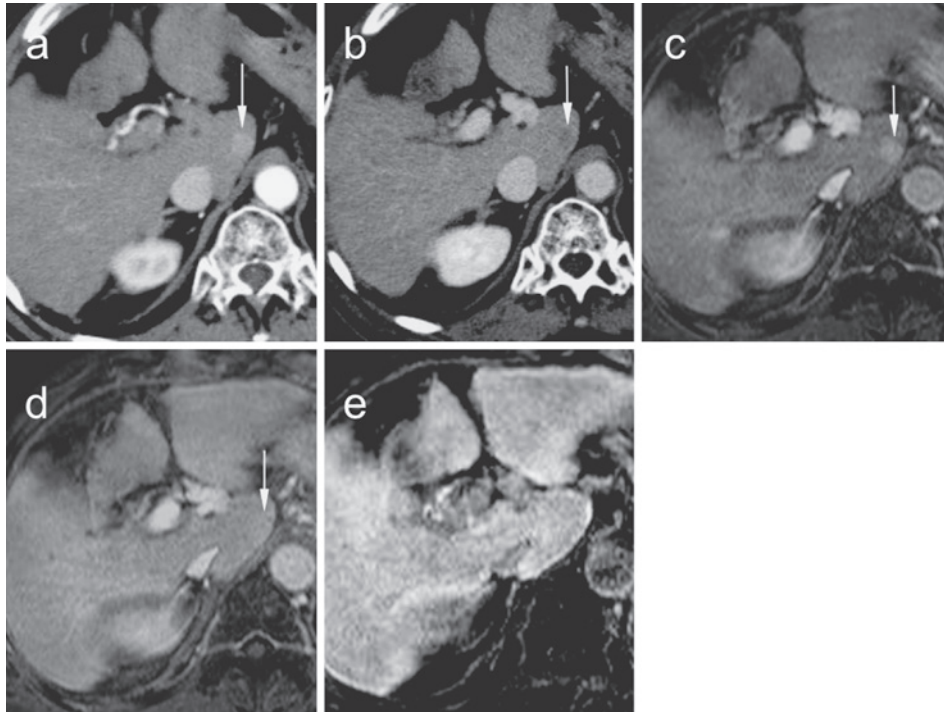


Fig. 2 A 76-year-old man with multiple HCC lesions.

- A contrast-enhanced CT scan during the arterial phase shows a 1.5-cm-diameter hypervascular HCC lesion in segment I (arrow).
- A contrast-enhanced CT scan during the equilibrium phase shows the washout pattern of HCC in segment I (arrow).
- A T1-weighted Gd-EOB-DTPA-enhanced arterial phase MR image shows a hypervascular nodule in segment I (arrow).
- A T1-weighted Gd-EOB-DTPA-enhanced equilibrium phase MR image shows no lesion in segment I (arrow).
- A T1-weighted Gd-EOB-DTPA-enhanced hepatobiliary phase MR image shows no lesion in segment I (false-negative lesion on MRI).

HCC: hepatocellular carcinoma, CT: computed tomography, Gd-EOB-DTPA: gadolinium-ethoxybenzyl-diethylenetriamine-pentaacetic acid, MR: magnetic resonance

93% (56 of 60), respectively, for Gd-EOB-DTPA-enhanced MRI.

## Discussion

With its superior spatial and temporal resolution, multislice CT has improved detection and characterization of focal liver lesions. In the diagnosis of HCC, multislice CT has proven to be robust and reliable.<sup>5,6)</sup> Nevertheless, some studies suggest that MRI is the most sensitive and specific technique for evaluating the liver.<sup>26,27)</sup>

Gd-EOB-DTPA is a novel liver-specific MRI contrast agent that acts as both an extracellular and hepatocyte-targeted agent. Our study was designed to compare the ability of 2 imaging modalities to detect HCC in a routine clinical setting. We included all patients with suspected focal liver lesions revealed by US, unenhanced CT, or ele-

vated serum  $\alpha$ -fetoprotein levels. Because 10% to 20% of HCC develops in noncirrhotic liver or in patients with non-viral hepatitis—or is incidental thereto<sup>2,19)</sup>—we included patients with or without known hepatic disease. Gd-EOB-DTPA-enhanced MRI, which had a sensitivity of 93%, was significantly more accurate than dynamic-enhanced CT, which had a sensitivity of 74%. The sensitivity of CT in detecting HCC was a little lower in our study than in previous studies.<sup>15,16)</sup> Both scanning time after administration of contrast media and flow rate were fixed in all the present patients, which might have decreased the detection rate of CT in our study. The discrepancy in detection rate was confirmed on blinded reading, *i.e.*, interpretation without knowledge of clinical findings or the results of other imaging examinations. Additionally, our results regarding the diagnostic accuracy of the 2 modalities compare favorably

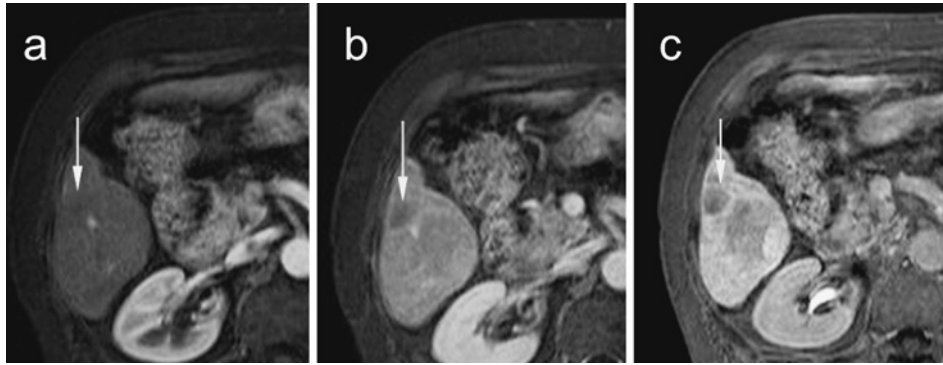


Fig. 3 A 73-year-old woman with multiple HCC lesions.

a. A T1-weighted Gd-EOB-DTPA-enhanced arterial phase MR image shows no hypervascular lesion in segment VI (arrow).

b. A T1-weighted Gd-EOB-DTPA-enhanced equilibrium phase MR image shows a washed-out nodule in segment VI (arrow).

c. A T1-weighted Gd-EOB-DTPA-enhanced hepatobiliary phase MR image shows a hypointense nodule in segment VI (arrow) (false-positive lesion on MRI).

HCC: hepatocellular carcinoma, Gd-EOB-DTPA: gadolinium-ethoxybenzyl-diethylenetriamine-pentaacetic acid, MR: magnetic resonance

with those of earlier clinical studies with large sample sizes (>50 lesions),<sup>13, 16, 28)</sup> perhaps due to the higher tumor-to-liver contrast that is possible with hepatocyte-selective MRI.<sup>29, 30)</sup> The 15 lesions that CT failed to detect in 5 of the present patients appeared as areas without contrast uptake during the hepatobiliary phase on Gd-EOB-DTPA-enhanced MRI. In addition, all lesions exhibited very weak enhancement during the arterial phase on Gd-EOB-DTPA-enhanced MRI. In these 5 patients, the dynamic-enhanced CT studies were performed, on average, only 10 days before Gd-EOB-DTPA-enhanced MRI. Because these 15 lesions exhibited no washout pattern during the equilibrium phase on dynamic-enhanced CT, the observers were unable to identify the HCC lesions.

There were 4 lesions in 2 patients that were detected by dynamic-enhanced CT but not by Gd-EOB-DTPA-enhanced MRI. Those nodules were hypervascular HCC lesions and showed early enhancement during the arterial phases and a washout pattern during the equilibrium phase, as compared with liver parenchyma, on dynamic-enhanced CT. When we retrospectively reviewed the 4 missed lesions on Gd-EOB-DTPA-enhanced MR images, all lesions were isointense during the hepatobiliary phase. In a previous study, moderately or poorly differentiated HCC showed no enhancement during the hepatobiliary phase of Gd-EOB-DTPA-enhanced MRI, whereas highly differentiated HCC did show enhancement during this phase.<sup>31)</sup>

A false-positive lesion on Gd-EOB-DTPA-enhanced MRI

exhibited a washout pattern during the dynamic phase and hypointensity during the hepatobiliary phase. On the basis of Gd-EOB-DTPA-enhanced MR images, the observers diagnosed differentiated HCC; however, postoperative pathologic analysis revealed nodular hyperplasia. A previous study reported that some dysplastic nodules are hypointense during the hepatobiliary phase, as are HCC lesions.<sup>32)</sup> We observed no significant difference between HCC lesions and dysplastic nodules in terms of enhancement ratio during the hepatobiliary phase. Dysplastic nodules are considered to be consistent with a diagnosis of adenomatous hyperplasia by the International Working Party of the World Congress of Gastroenterology,<sup>33)</sup> and nodular hyperplasia is regarded as a regenerative lesion rather than a dysplastic lesion. Another study revealed that only 2% of focal nodular hyperplasias were hypointense during the hepatobiliary phase.<sup>34)</sup> Such false-positive lesion findings suggest that nodular hyperplasia is hypointense during the hepatobiliary phase. Thus, misdiagnosing lesions that are hypointense during the hepatobiliary phase as HCC or precancerous lesions could lead to overtreatment of benign lesions.

Recent multicenter trials showed that Gd-EOB-DTPA-enhanced MRI was better than unenhanced MRI in detecting lesions.<sup>35, 36)</sup> In addition, Gd-EOB-DTPA-enhanced MRI had better sensitivity and fewer false-positives than spiral CT, especially for lesions smaller than 1 cm.<sup>13)</sup> In a phase III multicenter trial in the United States, a 1.5-T

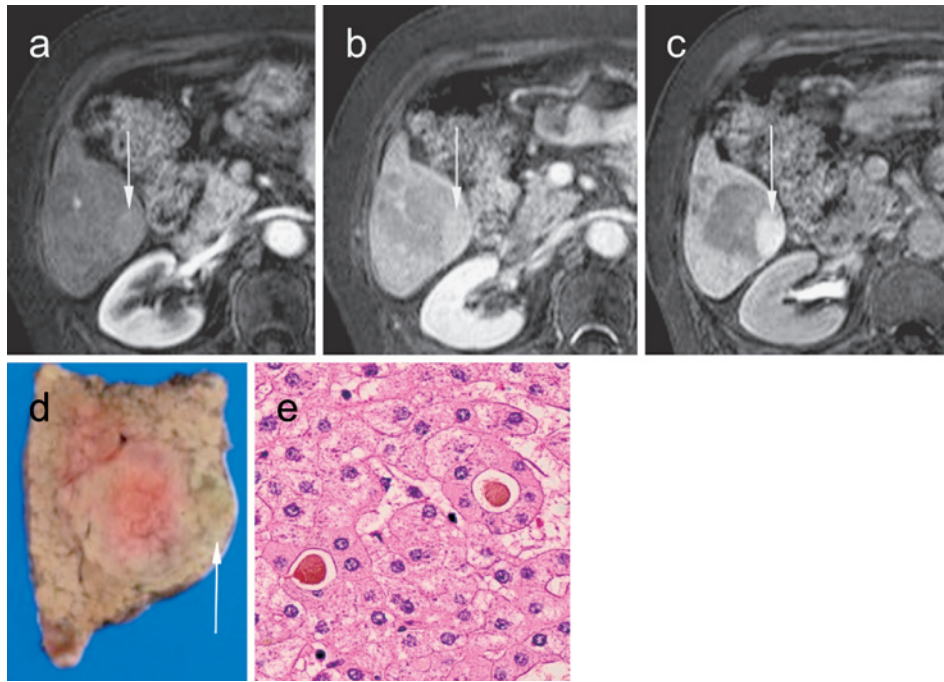


Fig. 4 A 73-year-old woman with multiple HCC lesions (same patient as in Fig. 3).

Histopathologic analysis of tissue obtained at biopsy (because of enlargement of this nodule in December 2006 and June 2007) revealed no malignant tumor cells. The diameter of the nodule increased from 24 mm to 40 mm in 2 years. The serum  $\alpha$ -fetoprotein level increased to 31 ng/ml. The patient's serum was negative for HCV antibody (anti-HCV), hepatitis B surface antigen (HBsAg), and hepatitis B core antibody (anti-HBc).

a. A T1-weighted Gd-EOB-DTPA-enhanced arterial phase MR image shows a focal hypervascular lesion (arrow) within the large hypovascular tumor in segment VI.

b. A T1-weighted Gd-EOB-DTPA-enhanced equilibrium phase MR image shows the weakly enhanced left inner part (arrow) of a large hypovascular tumor in segment VI.

c. A T1-weighted Gd-EOB-DTPA-enhanced hepatobiliary phase MR image shows a clear hypervascular lesion in the hypointense mass.

d. Grossly, the left inner part of the mass is greenish-brown and was thus designated a green hepatoma.

e. Histologically, the large mass in segment VI was a well-differentiated HCC characterized by fatty change and mild cell atypia. The greenish-brown part was also well-differentiated HCC characterized by pseudoglandular formation containing bile pigment (HE stain,  $\times 400$ ), which is a characteristic of green hepatoma. Normal liver parenchyma was present between these different areas.

HCC: hepatocellular carcinoma, HCV: hepatitis C virus, Gd-EOB-DTPA: gadolinium-ethoxybenzyl-diethylenetriamine-pentaacetic acid, MR: magnetic resonance, HE: hematoxylin and eosin

MRI was used to determine if Gd-EOB-DTPA-enhanced MRI was better than both unenhanced scans and standard dual-phase spiral CT for hepatic lesion characterization and classification, both clinically and in independent blinded reader evaluation. The authors of that study concluded that Gd-EOB-DTPA-enhanced MRI was safe and significantly improved the characterization and classification of a variety of focal hepatic lesions, as compared with unenhanced MRI and dual-phase spiral CT.<sup>16)</sup> A Japanese

phase III multicenter comparison of Gd-EOB-DTPA-enhanced MRI and contrast-enhanced CT, predominantly in patients with HCC and chronic liver disease,<sup>28)</sup> came to a similar conclusion.<sup>16)</sup>

We observed a green hepatoma that showed paradoxical uptake of contrast agent during the hepatobiliary phase. Studies have reported that some types of lesions are hyperintense during the hepatobiliary phase. In an analysis of liver-specific enhancement with Gd-EOB-

Table 1 Detection of HCC by dynamic contrast-enhanced CT and Gd-EOB-DTPA-enhanced MRI

Detected HCC (58 lesions)	Sensitivity (%)	Specificity (%)	Accuracy (%)
Dynamic-enhanced CT	74	100	91
Gd-EOB-DTPA-enhanced MRI	93	98	96

\*p&lt;0.05

HCC: hepatocellular carcinoma, CT: computed tomography, Gd-EOB-DTPA: gadolinium-ethoxybenzyl-diethylenetriamine-pentaacetic acid, MRI: magnetic resonance imaging

DTPA, hepatocyte-selective uptake was observed at 10 and 20 minutes after injection in a subset of focal nodular hyperplasia, adenoma, cystadenoma, and highly differentiated HCC, although moderately or poorly differentiated HCC lesions show no uptake, *i.e.*, the tumor was hypointense in comparison with normal liver parenchyma.<sup>31)</sup> Another study reported that all degrees of differentiated HCC could appear as iso- or hyperintense as compared with normal liver parenchyma during the hepatobiliary phase.<sup>17)</sup> Recently, Lee et al.<sup>37)</sup> reported no difference in bile production between non-hypointense and hypointense areas of HCC nodules. However, Tsuboyama et al.<sup>38)</sup> reported that HCC nodules with bile pigment showed higher enhancement during the hepatobiliary phase. Thus, the correlation between bile stasis and uptake of contrast agent remains unclear.

Recent reports have attempted to describe the molecular mechanism of Gd-EOB-DTPA transport into hepatocytes. Gd-EOB-DTPA is initially transported into hepatocytes via organic anion transporting polypeptides (Oatp) 1 in rats<sup>39)</sup> and excreted into bile via multidrug resistance-associated protein 2 (MRP2).<sup>40)</sup> A recent study of the characteristics of Gd-EOB-DTPA-positive HCC lesions during the hepatobiliary phase clarified the relation between enhancement ratios and expression levels of the OATP1B3 protein.<sup>41)</sup> This transporter is expressed in human liver, and its function is to bring drugs from the sinusoids into hepatocytes. Expression of OATP1B3 was nearly absent in most HCC lesions that did not exhibit uptake of Gd-EOB-DTPA, and expression of MRP2 was not correlated with enhancement ratios or bile production. Tsuboyama et al. reported a significant correlation between OATP1B1 and/or -1b3 expression and relative enhancement ratio, but not between MRP2 expression and relative enhancement ratio.<sup>38)</sup> MRP2 is localized in the canalicular membrane and secretes non-bile salt organic anions into bile.<sup>42)</sup>

MRP3 is localized in the basolateral membrane<sup>43,44)</sup> and transports bile salts and xenobiotic compounds.<sup>45,46)</sup> In a previous study, MRP2 immunostaining was observed in 87% (33/38) of HCC samples, and MRP3 was detected in all examined HCC samples.<sup>47)</sup> MRP3 is also involved in drug transport. There is therefore a need for studies of the relationship between MRP3 expression and Gd-EOB-DTPA uptake, as residual Gd-EOB-DTPA in tumor cells could potentially be used to predict chemotherapy response. In our study, we did not investigate the transporter in any patients. Further investigation is needed, especially for cases of green hematoma.

There are limitations in the present study that warrant mention. First, not all lesions were pathologically confirmed as standard of reference (SOR), so it is possible that some small lesions were missed by both imaging modalities, which could lead to a loss of diagnostic accuracy, including "false positives" and "false negatives", in the results of both modalities. However, in a clinical setting, it is very difficult to perform biopsies of all lesions detected by CT or MRI, which is a weakness of our study. A prospective randomized controlled trial is needed to evaluate diagnostic accuracy as SOR; however, biopsies of benign liver lesions, such as hemangiomas or focal nodular hyperplasia, are not the standard of care and therefore not ethically justified. Second, we evaluated the diagnostic accuracy of CT and MRI in detecting HCC in a selected patient population with suspected focal liver lesions, which could have resulted in higher diagnostic performance. Third, other HCC lesions were detected among the 7 patients with false-negative lesions, so there is not necessarily an effect on therapeutic strategy if it is possible to find some HCC lesions, using both modalities. For instance, the same treatment would be recommended for 4 or more HCC lesions, according to the Evidence-Based Practice Guidelines proposed by the Japan Society of Hepatology.<sup>48)</sup> Fourth, the

sensitivity and accuracy of Gd-EOB-DTPA-enhanced MRI for HCC were significantly greater than those of dynamic-enhanced CT, although some HCC lesions were detected only by dynamic-enhanced CT. Gd-EOB-DTPA-enhanced MRI is not a perfect alternative to dynamic-enhanced CT because the correct number and size of HCC lesions influence the therapeutic strategy. Fifth, to avoid higher radiation exposure and needle displacement, the scanning delay time for arterial phase imaging was not determined by the bolus tracking technique, which could yield better results than those achieved with our study protocols.<sup>49)</sup>

In conclusion, Gd-EOB-DTPA-enhanced MRI was more sensitive and accurate than dynamic-enhanced CT in detecting HCC lesions in routine clinical practice. Lesion vascularity and signal intensity during the hepatobiliary phase of Gd-EOB-DTPA-enhanced MRI may lead to more accurate diagnosis and could allow selection of the optimal treatment.

**Conflict of interest:** None declared.

We are most grateful to Dr. Chiaki Nishimura, formerly professor of the Department of Medical Informatics, Toho University School of Medicine, for his advice regarding statistical analysis. We would also like to express our gratitude to Dr. Noriaki Kameda, formerly Director of the Department of Surgical Pathology, Toho University Sakura Medical Center, for his advice on histopathologic analysis, and to Drs. Noriko Kitamura, Shusuke Kasuya, Hideyasu Kudo, and Tomoya Nakatsuka, Department of Radiology, Toho University Sakura Medical Center, for their help in collecting imaging data.

## References

- 1) Parkin DM, Bray F, Ferlay J, et al.: Estimating the world cancer burden: Globocan 2000. *Int J Cancer* **94**: 153–156, 2001
- 2) Caldwell S, Park SH: The epidemiology of hepatocellular cancer: From the perspectives of public health problem to tumor biology. *J Gastroenterol* **44** (Suppl 19): 96–101, 2009
- 3) Kudo M: Hepatocellular carcinoma 2009 and beyond: From the surveillance to molecular targeted therapy. *Oncology* **75** (Suppl 1): 1–12, 2008
- 4) Pleguezuelo M, Germani G, Marelli L, et al.: Evidence-based diagnosis and locoregional therapy for hepatocellular carcinoma. *Expert Rev Gastroenterol Hepatol* **2**: 761–784, 2008
- 5) Ariff B, Lloyd CR, Khan S, et al.: Imaging of liver cancer. *World J Gastroenterol* **15**: 1289–1300, 2009
- 6) Zech CJ, Reiser MF, Herrmann KA: Imaging of hepatocellular carcinoma by computed tomography and magnetic resonance imaging: State of the art. *Dig Dis* **27**: 114–124, 2009
- 7) Bonaldi VM, Bret PM, Reinhold C, et al.: Helical CT of the liver: Value of an early hepatic arterial phase. *Radiology* **197**: 357–363, 1995
- 8) Murakami T, Kim T, Takahashi S, et al.: Hepatocellular carcinoma: Multidetector row helical CT. *Abdom Imaging* **27**: 139–146, 2002
- 9) Kim YK, Kwak HS, Kim CS, et al.: Hepatocellular carcinoma in patients with chronic liver disease: Comparison of SPIO-enhanced MR imaging and 16-detector row CT. *Radiology* **238**: 531–541, 2006
- 10) Pawluk RS, Tummala S, Brown JJ, et al.: A retrospective analysis of the accuracy of T2-weighted images and dynamic gadolinium-enhanced sequences in the detection and characterization of focal hepatic lesions. *J Magn Reson Imaging* **9**: 266–273, 1999
- 11) Hamm B, Staks T, Mühler A, et al.: Phase I clinical evaluation of Gd-EOB-DTPA as a hepatobiliary MR contrast agent: Safety, pharmacokinetics, and MR imaging. *Radiology* **195**: 785–792, 1995
- 12) Reimer P, Rummeny EJ, Shamsi K, et al.: Phase II clinical evaluation of Gd-EOB-DTPA: Dose, safety aspects, and pulse sequence. *Radiology* **199**: 177–183, 1996
- 13) Hammerstingl R, Huppertz A, Breuer J, et al.: Diagnostic efficacy of gadoxetic acid (Primovist)-enhanced MRI and spiral CT for a therapeutic strategy: Comparison with intraoperative and histopathologic findings in focal liver lesions. *Eur Radiol* **18**: 457–467, 2008
- 14) Mita K, Kim SR, Kudo M, et al.: Diagnostic sensitivity of imaging modalities for hepatocellular carcinoma smaller than 2 cm. *World J Gastroenterol* **16**: 4187–4192, 2010
- 15) Halavaara J, Breuer J, Ayuso C, et al.: Liver tumor characterization: Comparison between liver-specific gadoxetic acid disodium-enhanced MRI and biphasic CT—A multicenter trial. *J Comput Assist Tomogr* **30**: 345–354, 2006
- 16) Raman SS, Leary C, Bluemke DA, et al.: Improved characterization of focal liver lesions with liver-specific gadoxetic acid disodium-enhanced magnetic resonance imaging: A multicenter phase 3 clinical trial. *J Comput Assist Tomogr* **34**: 163–172, 2010
- 17) Kim SH, Kim SH, Lee J, et al.: Gadoxetic acid-enhanced MRI versus triple-phase MDCT for the preoperative detection of hepatocellular carcinoma. *AJR Am J Roentgenol* **192**: 1675–1681, 2009
- 18) Jung G, Breuer J, Poll LW, et al.: Imaging characteristics of hepatocellular carcinoma using the hepatobiliary contrast agent Gd-EOB-DTPA. *Acta Radiol* **47**: 15–23, 2006
- 19) Leone N, Volpes R, Carrera M, et al.: Hepatocellular carcinoma in a non-cirrhotic liver. Two case reports and literature review. *Panminerva Med* **42**: 151–154, 2000
- 20) Bartolozzi C, Crocetti L, Lencioni R, et al.: Biliary and reticuloendothelial impairment in hepatocarcinogenesis: The diagnostic role of tissue-specific MR contrast media. *Eur Radiol* **17**: 2519–2530, 2007
- 21) Kanematsu M, Goshima S, Kondo H, et al.: Optimizing scan delays of fixed duration contrast injection in contrast-enhanced biphasic multidetector-row CT for the liver and the detection of hypervascular hepatocellular carcinoma. *J Comput Assist Tomogr* **29**: 195–201, 2005
- 22) Silverman PM, Kohan L, Ducic I, et al.: Imaging of the liver with helical CT: A survey of scanning techniques. *AJR Am J Roentgenol* **170**: 149–152, 1998
- 23) Yamashita Y, Komohara Y, Takahashi M, et al.: Abdominal helical CT: Evaluation of optimal doses of intravenous contrast material—A prospective randomized study. *Radiology* **216**: 718–723, 2000
- 24) Heiken JP, Brink JA, McClennan BL, et al.: Dynamic incremental CT: Effect of volume and concentration of contrast material and

- patient weight on hepatic enhancement. *Radiology* **195**: 353–357, 1995
- 25) Brink JA, Heiken JP, Forman HP, et al: Hepatic spiral CT: Reduction of dose of intravenous contrast material. *Radiology* **197**: 83–88, 1995
  - 26) Teefey SA, Hildeboldt CC, Dehdashti F, et al: Detection of primary hepatic malignancy in liver transplant candidates: Prospective comparison of CT, MR imaging, US, and PET. *Radiology* **226**: 533–542, 2003
  - 27) Kim MJ, Choi JY, Chung YE, et al: Magnetic resonance imaging of hepatocellular carcinoma using contrast media. *Oncology* **75** (Suppl 1): 72–82, 2008
  - 28) Ichikawa T, Saito K, Yoshioka N, et al: Detection and characterization of focal liver lesions: A Japanese phase III, multicenter comparison between gadoxetic acid disodium-enhanced magnetic resonance imaging and contrast-enhanced computed tomography predominantly in patients with hepatocellular carcinoma and chronic liver disease. *Invest Radiol* **45**: 133–141, 2010
  - 29) Ni Y, Marchal G: Enhanced magnetic resonance imaging for tissue characterization of liver abnormalities with hepatobiliary contrast agents: An overview of preclinical animal experiments. *Top Magn Reson Imaging* **9**: 183–195, 1998
  - 30) Ni Y, Marchal G, Yu J, et al: Prolonged positive contrast enhancement with Gd-EOB-DTPA in experimental liver tumors: Potential value in tissue characterization. *J Magn Reson Imaging* **4**: 355–363, 1994
  - 31) Huppertz A, Haraida S, Kraus A, et al: Enhancement of focal liver lesions at gadoxetic acid-enhanced MR imaging: Correlation with histopathologic findings and spiral CT—Initial observations. *Radiology* **234**: 468–478, 2005
  - 32) Saito K, Kotake F, Ito N, et al: Gd-EOB-DTPA enhanced MRI for hepatocellular carcinoma: Quantitative evaluation of tumor enhancement in hepatobiliary phase. *Magn Reson Med Sci* **4**: 1–9, 2005
  - 33) International Working Party: Terminology of nodular hepatocellular lesions. *Hepatology* **22**: 983–993, 1995
  - 34) Zech CJ, Grazioli L, Breuer J, et al: Diagnostic performance and description of morphological features of focal nodular hyperplasia in Gd-EOB-DTPA-enhanced liver magnetic resonance imaging: Results of a multicenter trial. *Invest Radiol* **43**: 504–511, 2008
  - 35) Bluemke DA, Sahani D, Amendola M, et al: Efficacy and safety of MR imaging with liver-specific contrast agent: U.S. multicenter phase III study. *Radiology* **237**: 89–98, 2005
  - 36) Huppertz A, Balzer T, Blakeborough A, et al: Improved detection of focal liver lesions at MR imaging: Multicenter comparison of gadoxetic acid-enhanced MR images with intraoperative findings. *Radiology* **230**: 266–275, 2004
  - 37) Lee S, Kim SH, Park CK, et al: Comparison between areas with Gd-EOB-DTPA uptake and without in hepatocellular carcinomas on Gd-EOB-DTPA-enhanced hepatobiliary-phase MR imaging: Pathological correlation. *J Magn Reson Imaging* **32**: 719–725, 2010
  - 38) Tsuboyama T, Onishi H, Kim T, et al: Hepatocellular carcinoma: Hepatocyte-selective enhancement at gadoxetic acid-enhanced MR imaging—Correlation with expression of sinusoidal and canalicular transporters and bile accumulation. *Radiology* **255**: 824–833, 2010
  - 39) van Montfoort JE, Stieger B, Meijer DK, et al: Hepatic uptake of the magnetic resonance imaging contrast agent gadoxetate by the organic anion transporting polypeptide Oatp1. *J Pharmacol Exp Ther* **290**: 153–157, 1999
  - 40) Pascolo L, Petrovic S, Cupelli F, et al: Abc protein transport of MRI contrast agents in canalicular rat liver plasma vesicles and yeast vacuoles. *Biochem Biophys Res Commun* **282**: 60–66, 2001
  - 41) Narita M, Hatano E, Arizono S, et al: Expression of OATP1B3 determines uptake of Gd-EOB-DTPA in hepatocellular carcinoma. *J Gastroenterol* **44**: 793–798, 2009
  - 42) Paulusma CC, Oude Elferink RP: The canalicular multispecific organic anion transporter and conjugated hyperbilirubinemia in rat and man. *J Mol Med (Berl)* **75**: 420–428, 1997
  - 43) Bodo A, Bakos E, Szeri F, et al: Differential modulation of the human liver conjugate transporters MRP2 and MRP3 by bile acids and organic anions. *J Biol Chem* **278**: 23529–23537, 2003
  - 44) König J, Rost D, Cui Y, et al: Characterization of the human multidrug resistance protein isoform MRP3 localized to the basolateral hepatocyte membrane. *Hepatology* **29**: 1156–1163, 1999
  - 45) Kool M, van der Linden M, de Haas M, et al: MRP3, an organic anion transporter able to transport anti-cancer drugs. *Proc Natl Acad Sci USA* **96**: 6914–6919, 1999
  - 46) Borst P, de Wolf C, van de Wetering K: Multidrug resistance-associated proteins 3, 4, and 5. *Pflugers Arch* **453**: 661–673, 2007
  - 47) Nies AT, König J, Pfannschmidt M, et al: Expression of the multidrug resistance proteins MRP2 and MRP3 in human hepatocellular carcinoma. *Int J Cancer* **94**: 492–499, 2001
  - 48) Makuuchi M, Kokudo N, Arii S, et al: Development of evidence-based clinical guidelines for the diagnosis and treatment of hepatocellular carcinoma in Japan. *Hepatol Res* **38**: 37–51, 2008
  - 49) Dinkel HP, Fieger M, Knüpfper J, et al: Optimizing liver contrast in helical liver CT: Value of a real-time bolus-triggering technique. *Eur Radiol* **8**: 1608–1612, 1998

# Gd-EOB-DTPA 造影 MRI 検査の マルチスライスダイナミック CT 検査に対する 肝細胞癌検出能の優位性

笠井ルミ子<sup>1)</sup> 長谷部光泉<sup>2)</sup> 高田 伸夫<sup>3)</sup>  
稲岡 努<sup>1)</sup> 蛭田 啓之<sup>4)</sup> 寺田 一志<sup>1)</sup>

<sup>1)</sup>東邦大学医学部放射線医学講座 (佐倉)

<sup>2)</sup>東海大学医学部専門診療学系画像診断学/東海大学医学部附属八王子病院放射線科

<sup>3)</sup>東邦大学医学部内科学講座消化器内科学分野 (佐倉)

<sup>4)</sup>東邦大学医学部病院病理学講座 (佐倉)

## 要約

**目的:** 肝細胞特異性造影剤 (gadolinium-ethoxybenzyl-diethylenetriamine-pentaacetic acid : Gd-EOB-DTPA) を用いた造影 magnetic resonance imaging (MRI) (EOB-MRI) および dynamic computed tomography (CT) (64 列マルチスライス CT) の肝細胞癌検出能について比較検討した。

**方法:** 肝占拠性病変が疑われた 47 人の患者 (平均 65.4 歳 ± 9.1 歳) に対し, dynamic CT および EOB-MRI を 6 週間以内に施行. 専門医によりモダリティ別に画像診断を行い, 採血結果や病理学的組織診断を含むすべての臨床情報に基づいた診断結果と比較した. 病変基準での各モダリティの肝細胞癌検出能について統計学的解析 (McNemar 検定) を施行した.

**結果:** 24 人 (58 病変) の肝細胞癌が総合的に診断された. Dynamic CT および EOB-MRI で検出された結節数はそれぞれ, 43 結節・54 結節であり, 感度は EOB-MRI で有意に高かった (74%, 93%,  $p=0.022$ ). うち 39 結節は双方の modality で検出され, 15 結節は dynamic CT では検出されなかったが, EOB-MRI の肝細胞造影相にて EOB 取り込みが低下しており早期動脈相では非常に淡い早期濃染を認めた. また EOB-MRI 肝細胞造影相で EOB 取り込みの高い部位と低い部位が混在する結節が 1 例で認められ, 術後病理組織学的診断にて偽腺管構造およびその内部に胆汁うっ滞をみるいわゆる「green hepatoma」であった.

**結論:** Dynamic CT と比較して, EOB-MRI は有意に肝細胞癌の検出能が高かった. 両モダリティにて, 検出しえた結節と検出しえなかった結節がそれぞれ認められ, 肝細胞癌のサーベイランスアルゴリズムの更なる検討が必要であると考えられる.

東邦医学会誌 59(6): 279-289, 2012

索引用語: 肝細胞癌, Gd-EOB-DTPA, MRI, ダイナミック CT, 検出能